Multimodal method for 2D sloshing in a circular tank

Odd M. Faltinsen[1], Alexander Timokha
Dept. Marine Technology & Centre for Ships and Ocean Structures,
Norwegian University of Science and Technology,
NO-7491, Trondheim, Norway; odd.faltinsen@ntnu.no

1. Natural sloshing modes. Analytically-oriented multimodal methods exist when the exact analytical natural sloshing modes (a) are expandable over the mean free surface, (b) exactly satisfy the Laplace equation and the zero-Neumann condition on the wetted walls, and (c) admit higher-order derivatives on the mean free surface. Construction of approximate natural modes for a two-dimensional circular tank is discussed by Faltinsen & Timokha (2009). They showed, inspired by Barkowiak et al.'s (1985) experiments, that the velocity potential for a horizontal dipole in infinite fluid, i.e.

$$W_1(y,z) = 2y \,/\, \left(y^2 + (z-a)^2\right), \tag{1}$$

approximates the first antisymmetric natural mode φ_1. Here the origin of the Oyz-plane lies in the circle centre, z is directed upwards, and a is the vertical dipole position. The dipole-type solution satisfies the Laplace equation, the liquid volume conservation condition, and, if $a = R_0$ with R_0 as the radius, the Neumann boundary condition on the wetted walls for any tank fillings. An approximate natural frequency was obtained by using the Rayleigh quotient variational formulation. When the depth-to-tank radius ratio $\overline{h} = h \,/\, R_0 \le 1$, the solution (1) gives only 1% larger numerical values than those by McIver (1989); moreover, a is then close to R_0. For larger depths, $1 < \overline{h} < 2$, the dipole-type solution leads to a larger difference from McIver's results. For instance, the depth $\overline{h} = 1.8$ leads to about 5% error with $a = 1.227R_0$.

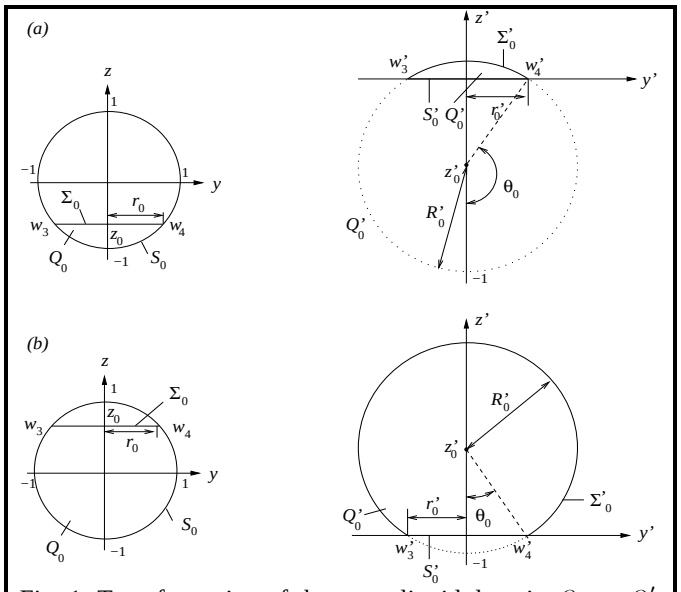

Fig. 1: Transformation of the mean liquid domain Q_0 to Q_0' for lower ($h \,/\, R_0 < 1$, (a)) and higher ($h \,/\, R_0 > 1$, (b)) depths; $h \,/\, R_0 = z_0 + 1$.

Three questions to be answered are: *(i) What could be a generalization of the dipole-type approximation for the higher natural sloshing modes? (ii) How to make the dipole-type approximation more precise, especially, for larger depths? (iii) Can these approximations be used in the multimodal methods?*

The whole R_0-scaled circular tank domain is conformally transformed to a half-plane so that the mean liquid domain maps to a circular segment, the transformed wetted tank surface becomes a chord lying on the horizontal axis, but the mean liquid surface maps to an arc lying in the upper half-plane (see, Fig. 1). The conformal transformation maps the eigenmodes φ_n to φ_n' so that they are invariant in satisfying the Laplace equation, and the zero-Neumann boundary conditions on S_0 and S_0'. The mean free surface (chord) Σ_0 transforms to the circular segment Σ_0' so that the spectral condition $\partial\varphi_n \,/\, \partial n = \kappa_n\varphi_n$ maps to $\partial\varphi_n' \,/\, \partial n' = \kappa_n(1-z_0)\varphi_n \,/\, (1+z')$. Any z'-even harmonic function in the transformed plane has the original in the physical plane which satisfies conditions (a) and (b) stated in the beginning. The image of (1) with $a = 1$ is the linear polynomials $W_1' = y'$ in the transformed plane. The analogy of the dipole-type approximation for the higher natural modes is the following set of the so-called harmonic polynomials (`regular' coordinate functions in the transformed plane)

$$W_i'(y',z') = \sum_{k=0}^{[i/2]} (-1)^k C_i^{2k} y'^{i-2k} z'^{2k} \quad (i = 0,1,...); \quad C_i^{2k} = (2k)!/\,(i!(2k-i)!), \tag{2}$$

($[i \,/\, 2]$ is the integer part of $i \,/\, 2$) and considering their originals

[1] Presenting author

$$W_0(y,z)=1;\quad W_1(y,z)=\frac{2y}{y^2+(z-1)^2};\ W_2(y,z)=\frac{2y^2+(y^2+z^2+1)^2}{\left(y^2+(z-1)^2\right)^2}=2\frac{\partial W_1}{\partial y}-2V_1-1;\ldots. \qquad (3)$$

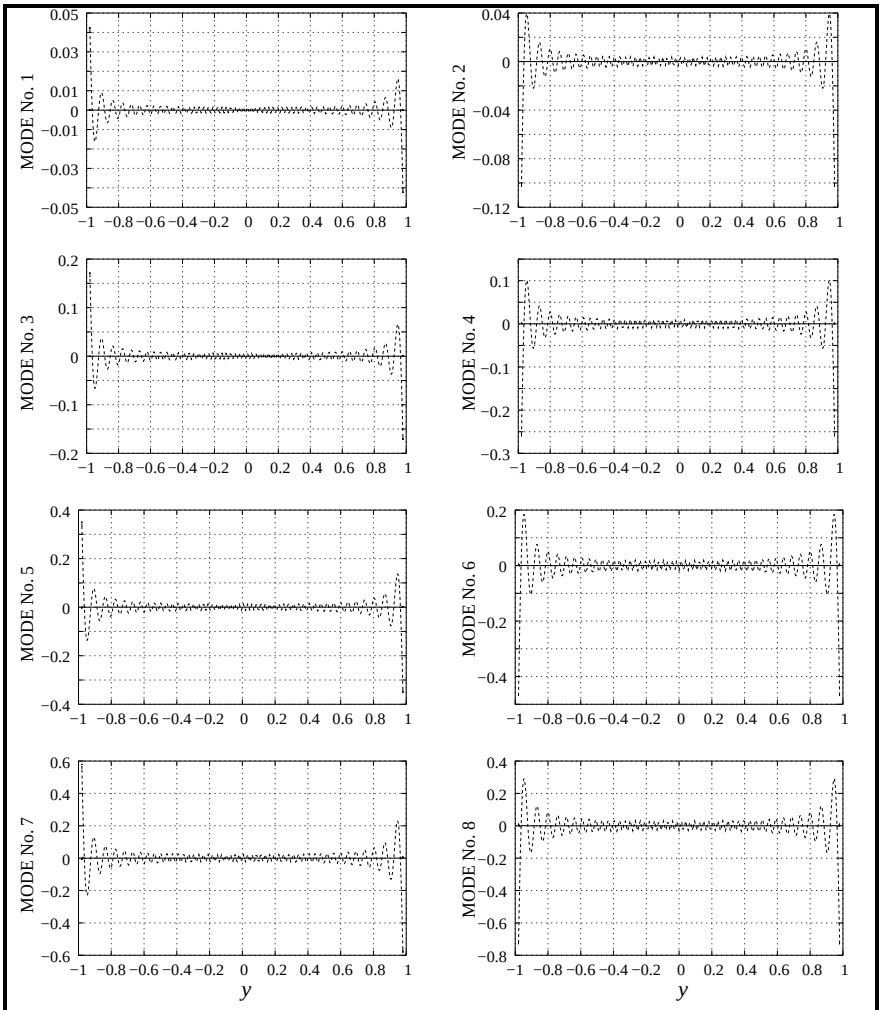

Fig. 2: Typical relative error in satisfying the spectral boundary condition on Σ_0 for middle depths, $0.8 < h\,/\,R_0 \le 1.25$. The Treftz solution is based on `regular' coordinate functions (dotted line, $q_1 = 50$), and the use of the correcting `singular' functions ($q_1 = 50,\ q_2 = 2$, solid line); $h\,/\,R_0 = 1.2$ and q_1, q_2 are defined by (4). The maximum uniform error with correcting functions is established for the eight mode; it is of the order 10^{-3} (hardly seen in the graphs). This error for the lowest mode is of the order 10^{-5}.

Here $V_1 = 2(z-1)\,/\,(y^2+(z-1)^2)$ is a vertical dipole in the physical plane.

The natural modes have a `singular' asymptotic behavior at the corner points $w_3$ and $w_4$ between $\Sigma_0$ and $S_0$ (Fig. 1). For $1 < h\,/\,R_0 < 2$, the inner angle at this corner point exceeds $\frac{1}{2}\pi$ and this asymptotics causes infinite second-order derivatives. Correcting `singular' harmonic functions ϕ_i' are analytically defined in the transformed plane[2]. The originals of these functions exactly satisfy the zero-Neumann boundary condition on S_0 and possess the needed singular asymptotics.

The `regular' and `singular' coordinate functions are combined in the Treftz variational method as

$$\varphi_n'(y',z') = \sum_{i=0}^{q} c_i \Phi_i'(y',z'),$$

where c_i are unknown weight coefficients, and the coordinate functions are

$$\Phi_0' = W_0',\ \Phi_1' = W_1',\ldots,\ \Phi_{q_1}' = W_{q_1}';\ \Phi_{q_1+1}' = \phi_1',\ \Phi_{q_1+2}' = \phi_2',\ldots,\ \Phi_{q_1+q_2+1}' = \phi_{q_2}' \quad (q = q_1+q_2+1) \qquad (4)$$

to be substituted into the Rayleigh quotient (Faltinsen & Timokha, 2009). The original spectral boundary problem is reduced to a matrix spectral problem with respect to the eigenvalues κ_n and the orthogonal eigenvectors $(c_0, c_1, \ldots, c_q)$. Vekua (1953,1967) proved that the harmonic polynomials constitute a complete set of functions in the corresponding metrics. Numerical analysis confirms that, as long as $0 < h\,/\,R_0 \le 1$, using this Treftz method gives an accurate approximation of the natural sloshing modes with *dominant contribution* of the `regular' coordinate function $W_n'$ to the eigenfunction $\varphi_n'$. Moreover, for smaller depths, $0 < h\,/\,R_0 \le 0.8$, the free-surface condition is uniformly approximated. The use of a pure `regular' basis is not possible for higher liquid depths. Using a few correcting `singular' functions ϕ_i' makes it possible to get accurate natural modes and uniformly approximate the free-surface condition for $0.8 < h\,/\,R_0 \le 1.25$ as illustrated in Fig. 2.

[2] The exact mathematical expressions for these `correcting' functions are rather massive to be included into this four-page presentation.

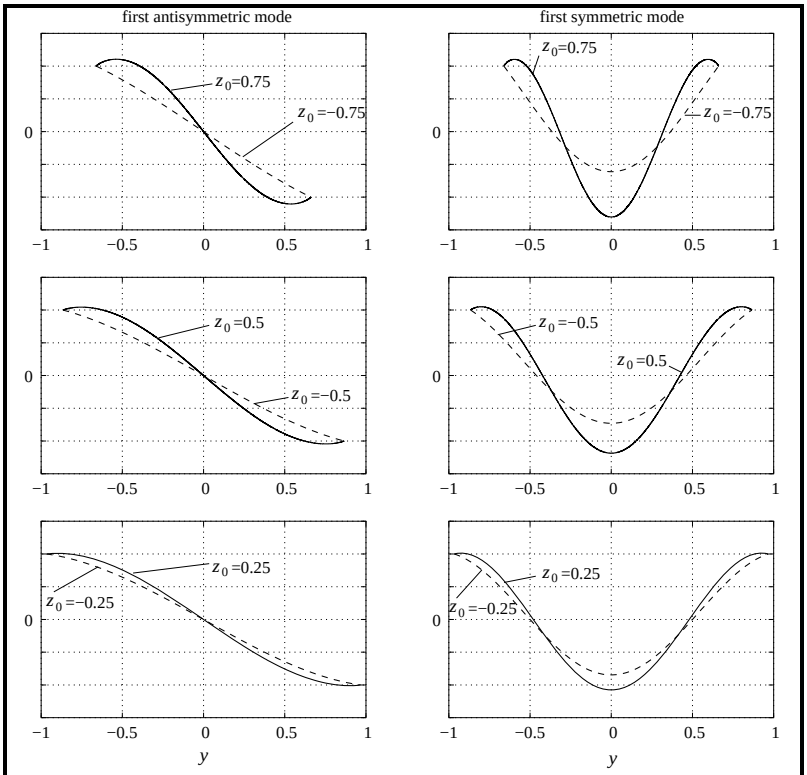

Fig. 3: The eigenmode wave profiles are normalized to provide the same elevation at the end. The first antisymmetric mode corresponds to $\kappa_1 = \sigma_1^2 / g$, but the first symmetric mode implies κ_2; $z_0 = h / R_0 - 1$. For $h / R_0 > 1$, the local extrema are inside of Σ_0.

The method requires more correcting functions to reach the needed accuracy for larger depths, $1.25 < h / R_0 \le 1.95$. The eigenvalue results are consistent with numerical values by McIver (1989) and require less strict requirements in uniformly satisfying the free surface condition than the eigenmodes. Unfortunately, McIver did not present the eigenmode results. The constructed approximate natural modes satisfy conditions (a)-(c) stated in the beginning.

Because the approximate natural modes are very accurate at the corner points, we are able to illustrate (Fig. 3) the `high spots' theorem by Kulczycki & Kuznetsov (2009) which states that the maximum wave elevation of the lowest mode occurs away from the tank wall when the inner corner angle exceeds $\frac{1}{2}\pi$. The absolute value of the wave slope at the tank wall for $z_0 > 0$ increases with increasing z_0 and tends to infinity when $z_0 \to 1$. Fig. 3 also shows that, for smaller depths, the first antisymmetric mode has close to a linear character, i.e. the eigenoscillations can be approximated by $y \cos\left(\sigma_1 t\right)$.

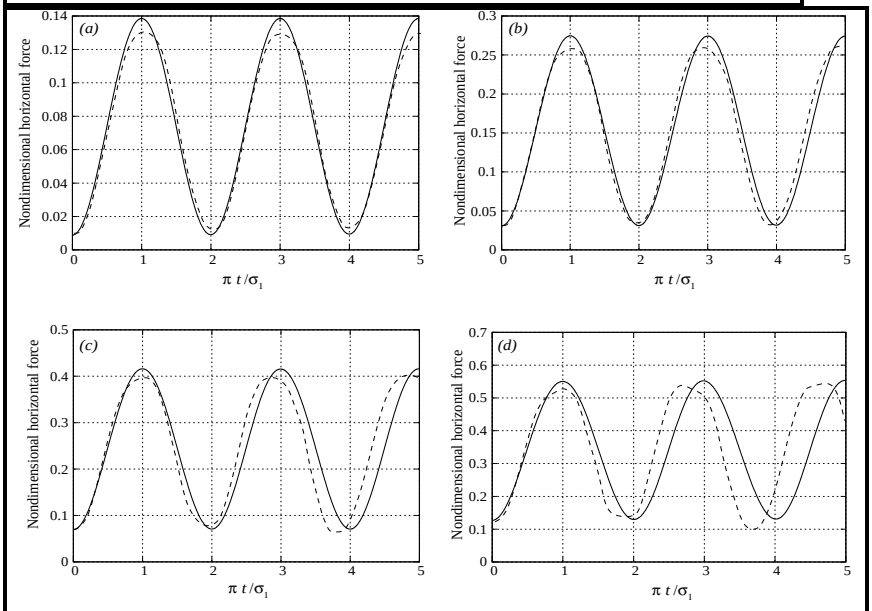

Fig 4: Nondimensional horizontal hydrodynamic force $F_2(t) / [\rho L_1 (2R_0)^2 \ddot{\eta}_{2a}]$ for the left turning of a lorry tank containing water with the constant horizontal acceleration $\ddot{\eta}_{2a} = 0.0408\, g$ simulated by Aliabadi et al. (2003) (dashed line) for $2R_0 = 1\,\mathrm{m}$ by using a fully nonlinear viscous 3D FEM method; L_1 is the longitudinal tank length. The solid lines represent results by the linear multimodal theory. (a) $h / R_0 = 0.3$, (b) $h / R_0 = 0.5$, (c) $h / R_0 = 0.7$, and (d) $h / R_0 = 0.9$.

2. Multimodal theory. To address question (iii), we adopt the approximate modes and construct the linear multimodal theory, linear modal equations and formula for linear potential-flow hydrodynamic force. There is no potential-flow hydrodynamic moment around an axis through O. The hydrodynamic coefficients needed in the multimodal theory can easily be calculated and tabled for later linear sloshing simulations.

For the transient case, the results by the linear multimodal theory are compared with the CFD-simulations by Aliabadi et al. (2003) (turning of a tanker vehicle with a constant nonzero acceleration) and Moderassi-Tehrani et al. (2006) (lane change of a tanker vehicle). The comparison supports applicability of the linear modal theory, but shows that free-surface nonlinearity may generally matter, especially for the higher liquid depths. Fig. 4 (d) illustrates this fact by different values of local maxima

and minima, and the corresponding time instants in fully nonlinear simulations by Aliabadi et al. (2003) relative to the linear sloshing theory. The time-behavior of linear theory is dominated by oscillations with σ_1, and shows negligible viscous boundary-layer damping effects. There is also difference (less than 15%) between our linear prediction and the nonlinear CFD-simulation by Moderassi-Tehrani et al. (2006) on the maximum hydrodynamic horizontal force, and the difference appears when the lane change time is close to the highest natural sloshing period. This difference may also be explained by nonlinearities by applying multimodal results for a rectangular tank. The contribution of higher modes is less than 1%, and viscous effects are negligible.

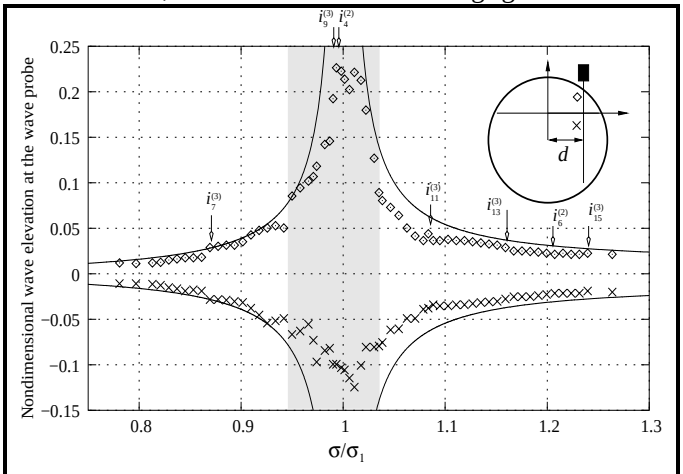

Fig. 5: Comparison between experimental data by Bogomaz & Sirota (2002) and the linear multimodal theory of the R_0-scaled steady-state (maximum and minimum) wave elevation at the wave probe situated at $d = 0.603777 R_0$; $R_0 = 0.1325$ m. The horizontal forcing amplitude is $0.0075472\, R_0$; $h / R_0 = 1.47$. The shadow zone is the frequency domain, where 3D waves occur. The secondary resonance due to the second-, third-order nonlinearities is indicated by $i_k^{(i)}$ (Faltinsen & Timokha, 2009), where k is the number of the corresponding mode, i is the order of nonlinearity.

For steady-state sloshing, results of the linear multimodal theory are compared with an experimental series by Bogomaz & Sirota (2002), who measured steady-state wave elevations away from the circular walls. The horizontal forcing amplitude was $0.0075472\, R_0$, and $h / R_0 = 1.47$ (Fig. 5). Because $R_0 = 0.1325\text{m}$ in the experiments, the surface tension is an error source relative to our theory. Bogomaz & Sirota (2002) discuss 3D phenomena similar to swirling for the shadow frequency domain. Far from this domain, the measurements support the linear multimodal theory, but there are several small `jumps' in the experimental responses which, as we show in the figure, can partly be explained by the secondary resonance phenomenon. The experimental series by Bogomaz & Sirota (2002) for the larger horizontal forcing amplitude $0.0203\ R_0$ does not support the linear sloshing theory. For these forcing amplitude, the experimental observations report strongly nonlinear waves with transition to three-dimensional sloshing for $0.85 \le \sigma / \sigma_1 \le 1.25$. Along with Bogomaz & Sirota (2002), strongly nonlinear resonant waves and overturning due to resonant excitation of the lowest natural frequency are reported by other authors. Example of the overturning waves due to resonant excitation of the first mode is presented by Kobayashi et al. (1989). How to construct a nonlinear multimodal theory for 2D sloshing in a circular tank will be discussed.

Aliabadi, S., Johnson, A., Abedi, J. (2003) Comparison of finite element and pendulum models for simulating of sloshing. *Computers & Fluids* **32**, 535-545.

Barkowiak, K., Gampert, B., and Siekmann, J. (1985) On liquid motion in a circular cylinder with horizontal axis. *Acta Mechanica* 54, 207–220.

Bogomaz, G.I. & Sirota S.A. (2002) *Oscillations of a liquid in containers: Methods and results of experimental studies*. Dnepropetrovsk: National Space Agency of Ukraine (in Russian).

Faltinsen, O.M., Timokha, A.N. (2009) *Sloshing*. Cambridge University Press.

Kobayashi, N., Mieda, T., Shiba, H., Shinozaki, Y. (1989) A study of the liquid slosh response in horizontal cylindrical tanks. *Transactions of the ASME. J. Pressure Vessel Technology* **111**, 32-38.

Kulczycki, T., Kuznetsov, N. (2009) `High spots' theorems for sloshing problems. *Bull. London Math. Soc*. **42**, 495-505.

McIver, P. (1989) Sloshing frequencies for cylindrical and spherical containers filled to an arbitrary depth. *J. Fluid Mech.* **201**, 243-357.

Moderassi-Tehrani, K., Rakheja, S., Sedaghati, R. (2006) Analysis of the overturning moment caused by transient liquid slosh inside a partly filled moving tank. *Proc. IMechE, Part D: Journal of Automobile Engineering* **220**, 289-301.

Vekua, I.A. (1953) On completeness of a system of harmonic polynomials in space. *Doklady Akad. Nauk SSSR (N.S.)* **90**, 495-498.

Vekua, I.A. (1967) *New methods for solving elliptic equations*. New York: Interscience Publishers John Wiley & Sons, Inc.